Check for updates

How to cite: *Angew. Chem. Int. Ed.* **2024**, *63*, e202402877
doi.org/10.1002/anie.202402877

NMR Spectroscopy | Hot Paper

Parahydrogen-Induced Polarization of ^{14}N Nuclei

Oleg G. Salnikov, Ivan A. Trofimov[+], Zachary T. Bender, Alexandra I. Trepakova, Jingyan Xu, Garrett L. Wibbels, Roman V. Shchepin,* Igor V. Koptyug, and Danila A. Barskiy**

Abstract: Hyperpolarization techniques provide a dramatic increase in sensitivity of nuclear magnetic resonance spectroscopy and imaging. In spite of the outstanding progress in solution-state hyperpolarization of spin-1/2 nuclei, hyperpolarization of quadrupolar nuclei remains challenging. Here, hyperpolarization of quadrupolar ^{14}N nuclei with natural isotopic abundance of >99 % is demonstrated. This is achieved via pairwise addition of parahydrogen to tetraalkylammonium salts with vinyl or allyl unsaturated moieties followed by a subsequent polarization transfer from ^{1}H to ^{14}N nuclei at high magnetic field using PH-INEPT or PH-INEPT+ radiofrequency pulse sequence. Catalyst screening identified water-soluble rhodium complex [Rh(P(*m*-$C_6H_4SO_3Na)_3)_3Cl$] as the most efficient catalyst for hyperpolarization of the substrates under study, providing up to 1.3 % and up to 6.6 % ^{1}H polarization in the cases of vinyl and allyl precursors, respectively. The performance of PH-INEPT and PH-INEPT+ pulse sequences was optimized with respect to interpulse delays, and the resultant experimental dependences were in good agreement with simulations. As a result, ^{14}N NMR signal enhancement of up to 760-fold at 7.05 T (corresponding to 0.15 % ^{14}N polarization) was obtained.

Nuclear magnetic resonance (NMR) spectroscopy and magnetic resonance imaging (MRI) are powerful techniques with various applications such as structural characterization of organic and inorganic compounds and biomolecules, mechanistic studies of chemical transformations, quantitative analysis, medical diagnostics etc. However, these techniques have a significant limitation of inherently low sensitivity resulting from low thermal polarization of nuclear spins. The efficient remedy for this issue is the use of hyperpolarization techniques which provide temporal increase of nuclear spin polarization up to several orders of magnitude.[1] The most widely used hyperpolarization techniques for solution-state NMR are dissolution dynamic nuclear polarization (dDNP),[2,3] parahydrogen-induced polarization (PHIP),[4–6] and signal amplification by reversible exchange (SABRE).[7–9] The latter two techniques use parahydrogen (p-H_2)—the singlet nuclear spin isomer of H_2—as a source of hyperpolarization. PHIP typically exploits pairwise addition of two H atoms from a p-H_2 molecule to the same substrate molecule using either homogeneous[10] or heterogeneous[11,12] hydrogenation catalysis, while in SABRE both p-H_2 and substrate molecules engage in reversible exchange with a metal complex, and polarization is transferred from p-H_2-derived hydrides to the substrate nuclei within the complex.

While originally PHIP and SABRE techniques were demonstrated for ^{1}H hyperpolarization, approaches for polarization transfer from protons to other spin-$^1/_2$ heteronuclei (e.g., ^{13}C or ^{15}N) were later developed.[13,14] Typically, these approaches follow one of the two strategies: (i) bringing the system to an appropriate magnetic field (typically on the order from hundreds of nanotesla to several microtesla) where protons and heteronuclei are strongly coupled with each other,[15–17] or (ii) application of dedicated radiofrequency (RF) pulse sequences at high magnetic field in an NMR spectrometer.[18–21]

The dominating majority of NMR-sensitive nuclei have spin $I > {}^1/_2$ and a quadrupolar moment, for example ^{2}H and ^{14}N ($I=1$), ^{11}B and ^{35}Cl ($I=3/2$), ^{17}O ($I=5/2$). The solution-

[*] Dr. O. G. Salnikov, I. A. Trofimov,[+] Dr. A. I. Trepakova, Prof. I. V. Koptyug
International Tomography Center SB RAS
3 A Institutskaya St., Novosibirsk 630090, Russia
E-mail: salnikov@tomo.nsc.ru

Z. T. Bender, G. L. Wibbels, Prof. R. V. Shchepin
South Dakota School of Mines & Technology
Rapid City, South Dakota 57701, United States
E-mail: Roman.Shchepin@sdsmt.edu

J. Xu, Dr. D. A. Barskiy
Helmholtz Institute Mainz, GSI Helmholtz Center for Heavy Ion Research GmbH, and
Institute of Physics, Johannes Gutenberg-Universität Mainz 55128, Germany
E-mail: dbarskiy@uni-mainz.de

[+] Current affiliation: Division of Medical Physics, Department of Diagnostic and Interventional Radiology, University Medical Center Freiburg, Faculty of Medicine, University of Freiburg, Freiburg 79106, Germany

© 2024 The Authors. Angewandte Chemie International Edition published by Wiley-VCH GmbH. This is an open access article under the terms of the Creative Commons Attribution License, which permits use, distribution and reproduction in any medium, provided the original work is properly cited.

© 2024 The Authors. Angewandte Chemie International Edition published by Wiley-VCH GmbH

state NMR of quadrupolar nuclei is challenging due to rapid quadrupolar relaxation resulting in a significant broadening of the NMR lines. To the best of our knowledge, there are only a few examples of quadrupolar nuclei hyperpolarization by PHIP so far, limited only to ^{2}H and ^{11}B. Aime et al. demonstrated spontaneous hyperpolarization of deuterium in ethylene-d_2 and ethane-d_4 produced via pairwise addition of p-H_2 to the corresponding unsaturated precursors at a low magnetic field (i.e., under ALTADENA[22] (adiabatic longitudinal transport after dissociation engenders net alignment) conditions) with polarization transfer mediated by ^{13}C nuclei present at natural abundance.[23] Additionally, ^{2}H nuclei can be polarized directly in the orthodeuterium-induced polarization (ODIP) experiments[24,25] which are conceptually similar to PHIP but use orthodeuterium as a source of spin order instead of p-H_2. Next, hyperpolarization of ^{11}B nuclei in aminoborane frustrated Lewis pairs was observed as a result of activation of p-H_2 and the application of PH-INEPT (parahydrogen–insensitive nuclei enhanced by polarization transfer) RF pulse sequence[26] or produced spontaneously for the reaction intermediates in alkyne hydrogenations catalyzed by these compounds.[27]

Nitrogen-14 is one of the most widespread quadrupolar nuclei (natural abundance of ^{14}N isotope is $>99\,\%$). Therefore, hyperpolarization of ^{14}N nuclei could potentially open the prospects for various applications in addition to fundamental interest. Herein, we explored the feasibility of hyperpolarization of ^{14}N nuclei using PHIP technique. As the symmetry of environment has a dramatic effect on the transverse relaxation time (T_2) of quadrupolar nuclei (and, hence, on the corresponding NMR linewidth), tetraalkylammonium salts with vinyl or allyl moieties were chosen as precursors for pairwise addition at high field (p-H_2) (PASADENA[4] (parahydrogen and synthesis allow dramatically enhanced nuclear alignment) experiment), producing hyperpolarized (HP) saturated tetraalkylammonium salts (Figure 1a). Pairwise addition of p-H_2 was followed by polarization transfer to ^{14}N nuclei at 7.05 T using PH-INEPT (Figure 1b) or PH-INEPT+ (Figure 1c) RF pulse sequence.

To the best of our knowledge, there are four publications on PHIP of tetraalkylammonium salts, which mostly employed ^{15}N-labeled compounds with the aim to transfer polarization to ^{15}N nuclei which possess exceptionally long ^{15}N longitudinal relaxation times (^{15}N T_1) of several minutes at high magnetic fields.[28–31] As most of these previous studies employed heterogeneous Rh metal nanoparticle catalysts, for the present study we chose heterogeneous Rh/TiO_2 catalyst as a starting point. This system catalyzed the formation of HP ethyltrimethylammonium bromide (ETMA) when corresponding trimethylvinylammonium (TMVA) precursor (80 mM) was employed. However, the product yield and polarization levels were not high enough for polarization transfer to ^{14}N (see Supporting Information for details, Figure S2). When the same catalyst was used for hydrogenation of allyltripropylammonium bromide (ATPA) with p-H_2, decomposition of the reactant to propylene and tripropylamine was observed while tetrapropylammonium was not formed at all (Figure S3). Therefore, we moved on to homogeneous catalysts with the goal to find the most efficient catalytic system for polarization transfer to ^{14}N nuclei in these compounds.

First, cationic [Rh(NBD)(dppb)]BF_4 complex (NBD = norbornadiene, dppb = 1,4-bis(diphenylphosphino)butane) showed no hydrogenation activity as it is likely deactivated by halide counterions of the tetraalkylammonium salts (see Figure S4 showing inhibition of propargyl alcohol hydrogenation upon addition of the halide). Next, the performance of Wilkinson's catalyst [Rh(PPh_3)$_3$Cl] was investigated. When TMVA was used as a substrate, PASADENA effects were observed for the formed ETMA, however, the corresponding ^{1}H NMR signals quickly disappeared (Figure S5). Instead, other PASADENA signals emerged which likely correspond to some saturated hydrocarbon. Moreover, the substrate solubility in organic solvent required to dissolve Wilkinson's catalyst was low. Hydrogenation of ATPA using Wilkinson's catalyst resulted in the reactant decomposition to tripropylamine and HP propylene similar to the case of Rh/TiO_2 (Figure S6). Next, we moved on to water-soluble analog of Wilkinson's catalyst [Rh(P(m-$C_6H_4SO_3Na$)$_3$)$_3$Cl] (**[Rh]$_{aq}$**). This catalyst allowed us to obtain ETMA with 0.57 % ^{1}H polarization and 23 % conversion of TMVA precursor under PASADENA conditions (Figure S8). Thus, **[Rh]$_{aq}$** catalyst was demonstrated to be the most efficient catalyst for polarization of ETMA among those tested in this study, and therefore, it was used in further experiments on polarization transfer to ^{14}N nuclei.

The preliminary trials of polarization transfer to ^{14}N using magnetic field cycling[15] approach were unsuccessful. Likely this is a result of rapid T_1 relaxation of ^{14}N nuclei at ultralow magnetic field inside the magnetic shield and at Earth's field (it is expected to be faster than relaxation at high field of 7.05 T reported below). Therefore, we next implemented high-field polarization transfer schemes based on the PH-INEPT RF pulse sequence. The choice of PH-INEPT was motivated by the fact that this sequence is relatively simple and it is easily adaptable to various spin systems.[32] The efficiency of polarization transfer using this approach strongly depends on the choice of interpulse delays.[33,34] The simulated dependence of PH-INEPT ^{14}N NMR signal of ETMA on the τ_1 delay is presented in

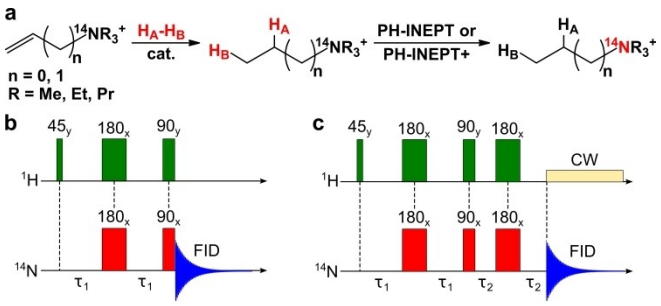

Figure 1. (a) Scheme of pairwise p-H_2 addition to unsaturated precursors producing HP saturated tetraalkylammonium salts with subsequent polarization transfer to ^{14}N nucleus using PH-INEPT or PH-INEPT+ pulse sequence. (b) Scheme of the PH-INEPT pulse sequence. (c) Scheme of the PH-INEPT+ pulse sequence with continuous wave (CW) proton decoupling.

© 2024 The Authors. Angewandte Chemie International Edition published by Wiley-VCH GmbH

15213773, 2024, 22, Downloaded from https://onlinelibrary.wiley.com/doi/10.1002/anie.202402877 by Universitätsbibliothek Mainz, Wiley Online Library on [24/04/2025]. See the Terms and Conditions (https://onlinelibrary.wiley.com/terms-and-conditions) on Wiley Online Library for rules of use; OA articles are governed by the applicable Creative Commons License

Figure 2c. According to simulations, the maximum ^{14}N polarization (in absolute values) is obtained at $\tau_1 = 50–53$ ms. For the experimental measurement of this dependence, the TMVA precursor concentration was increased from 80 mM to 400 mM and *p*-H_2 bubbling duration was decreased from 15 s to 7 s in order to perform multiple experiments on the same sample. Under these conditions, PASADENA ^1H polarizations reached ca. 1.1–1.3 % because of the reduced polarization losses due to relaxation effects (Figure 2a). The experimental PH-INEPT τ_1 sweep measurements were in overall good agreement with simulations—the positions and the signs of the maxima were well reproduced (Figure 2c). Here the sign of the ^{14}N signal signifies the appearance of its antiphase pattern—the absorption/emission patterns are taken to be positive while the emission/absorption patterns negative (see Figure S9 for the evolution of PH-INEPT ^{14}N NMR spectra of ETMA with τ_1 variation). There was a discrepancy in the relative intensities of the first two maxima, as the simulations predicted that the first maximum at $\tau_1 = 20–23$ ms should be ~2 times less intense than the second maximum at $\tau_1 = 50–53$ ms, while in the experimental measurements these maxima had similar absolute intensities. Because the relaxation effects were not considered in the simulations, this discrepancy can be attributed to the more pronounced relaxation losses at longer τ_1 delays. The highest experimentally obtained PH-INEPT ^{14}N signal enhancement factor for ETMA was 760, corresponding to 0.15 % ^{14}N polarization (Figure 2b).

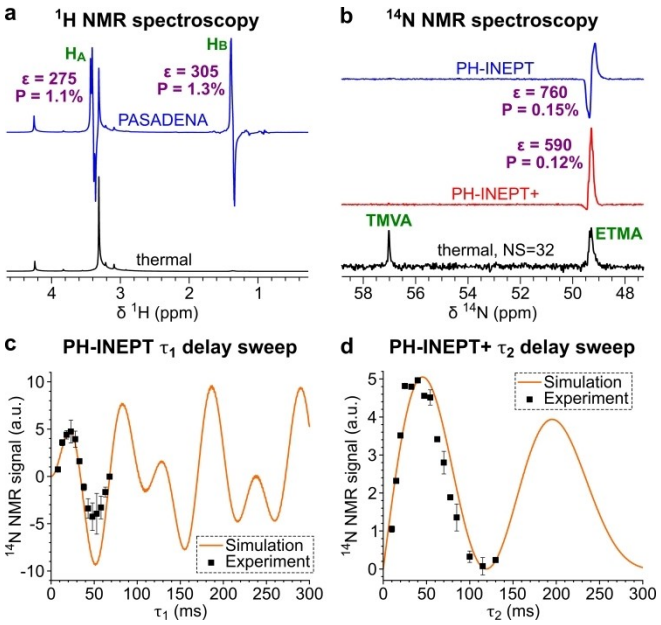

Figure 2. Results for ethyltrimethylammonium: (a) PASADENA ^1H NMR spectrum of ETMA (blue trace) and corresponding thermal ^1H NMR spectrum (black trace). Both spectra were acquired using 45° RF pulse. (b) ^{14}N NMR spectra: ETMA hyperpolarized using PH-INEPT RF pulse sequence with $\tau_1 = 53$ ms (blue trace), ETMA hyperpolarized using PH-INEPT+ RF pulse sequence with $\tau_1 = 53$ ms, $\tau_2 = 32.5$ ms (red trace), and thermally polarized reaction mixture after a series of 15 PH-INEPT experiments (black trace, 32 signal accumulations). (c) Experimental dependence of ETMA ^{14}N NMR signal on τ_1 delay of the PH-INEPT pulse sequence (black squares) and the corresponding simulated dependence (normalized to the experimental data, orange line). (d) Experimental dependence of ETMA ^{14}N NMR signal on τ_2 delay of the PH-INEPT+ pulse sequence (black squares) and the corresponding simulated dependence (normalized to the experimental data, orange line).

PH-INEPT pulse sequence results in an antiphase heteronuclear NMR signal which would be disadvantageous for MRI applications.[35] The required in-phase signal can be obtained by modification of PH-INEPT sequence by adding a refocusing block in the end (the resultant sequence is called PH-INEPT+[18]). Here, the optimization of PH-INEPT+ performance for ETMA was carried out in the same way as described previously for PH-INEPT. As the polarization transfer blocks in PH-INEPT and PH-INEPT+ pulse sequences are the same, the τ_1 value previously optimized for PH-INEPT can be safely used in PH-INEPT+ ,[33,34] leaving for optimization the value of τ_2 only. The performed simulations of τ_2 dependence of ^1H-decoupled PH-INEPT+ sequence predicted the broad maximum at $\tau_2 = 46$ ms (Figure 2d). This maximum was reproduced experimentally (Figure 2d). Minor horizontal shift of the simulated dependence by ca. 5–10 ms can be attributed to relaxation effects. The highest experimentally obtained PH-INEPT+ ^{14}N signal enhancement factor for ETMA was 590, corresponding to 0.12 % ^{14}N polarization (Figure 2b). The somewhat lower efficiency of PH-INEPT+ pulse sequence compared to PH-INEPT likely originates from the more pronounced relaxation effects in the case of the longer PH-INEPT+ sequence.

Next, the $\mathbf{[Rh]_{aq}}$ catalyst was examined in pairwise parahydrogen addition to allyltrimethylammonium bromide (ATMA) to form HP trimethylpropylammonium bromide (TMPA). In PASADENA experiment, ^1H polarizations of 4.4 % and 6.6 % were observed for methylene and methyl protons of TMPA, respectively (Figure 3a). The strong difference in polarization levels between these two groups of protons is mainly due to a higher multiplicity of the signal of the CH_2 group. As a result, hyperpolarization losses due to partial overlap of absorptive and emissive components of an antiphase PASADENA signal[34] (which were not taken into account) are more pronounced compared to the case of CH_3 protons. The obtained ^1H polarization levels are ca. 4–5 times higher than in the case of ETMA hyperpolarization under the same conditions. The simulated dependence of PH-INEPT ^{14}N NMR signal of TMPA on the τ_1 delay was in good agreement with experimental results (Figure 3c). The highest experimentally obtained PH-INEPT ^{14}N signal enhancement factor for TMPA was 240, corresponding to 0.05 % ^{14}N polarization (Figure 3b). The lower ^{14}N polarizations of TMPA compared to ETMA (despite the higher ^1H polarizations) can be attributed to less efficient PH-INEPT polarization transfer in TMPA. Indeed, while in ETMA both *p*-H_2-derived protons are *J*-coupled to ^{14}N nucleus, in TMPA $^4J_{NH}$ between the H_B proton (in the methyl group) and ^{14}N should be close to zero. More advanced polarization transfer schemes exploiting the transient polarization of α-CH_2 protons in TMPA as an intermediate site (similar to the proton-relayed approach

© 2024 The Authors. Angewandte Chemie International Edition published by Wiley-VCH GmbH

15213773, 2024, 22, Downloaded from https://onlinelibrary.wiley.com/doi/10.1002/anie.202402877 by Universitätsbibliothek Mainz, Wiley Online Library on [24/04/2025]. See the Terms and Conditions (https://onlinelibrary.wiley.com/terms-and-conditions) on Wiley Online Library for rules of use; OA articles are governed by the applicable Creative Commons License

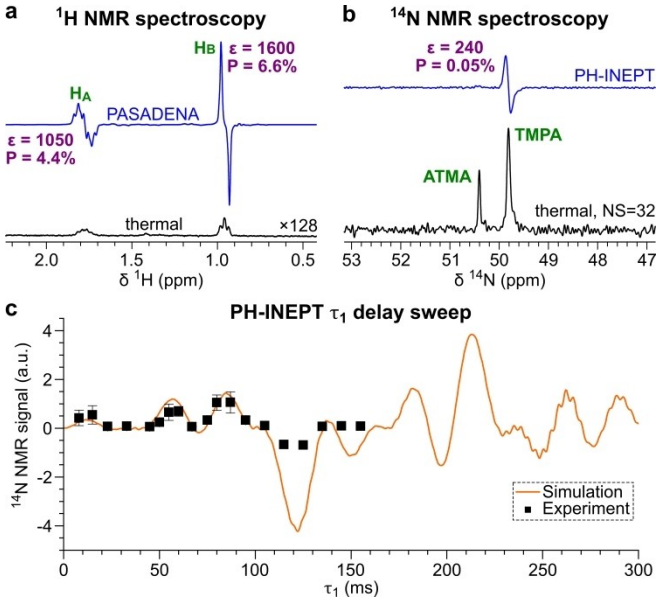

Figure 3. Results for trimethylpropylammonium: (a) PASADENA ^{1}H NMR spectrum of TMPA (blue trace) and the corresponding thermal ^{1}H NMR spectrum multiplied by a factor of 128 (black trace); the spectra were acquired using 45° RF pulse (the same spectra showing the full spectral range are presented in Figure S11). (b) ^{14}N NMR spectra: TMPA hyperpolarized using PH-INEPT RF pulse sequence with $\tau_1 = 87$ ms (blue trace), and thermally polarized reaction mixture after a series of 15 PH-INEPT experiments (black trace, 32 signal accumulations). (c) Experimental dependence of TMPA ^{14}N NMR signal on τ_1 delay of the PH-INEPT pulse sequence (black squares) and the corresponding simulated dependence (normalized to the experimental data, orange line).

recently reported for allyl esters[36]) are expected to provide a significant increase in ^{14}N polarization of this molecule.

^{14}N longitudinal relaxation times (T_1) were measured for the produced compounds in the reaction mixtures under H_2 pressure at 7.05 T field using inversion-recovery pulse sequence. The corresponding values were 3.0 ± 0.3 s for ETMA and 1.8 ± 0.2 s for TMPA, respectively (Figure S13). At the same time, ^{14}N T_1 of symmetric tetraethylammonium (TEA) bromide was 11 ± 1 s. Encouraged by this significant difference, we attempted to produce HP TEA by hydrogenation of the corresponding triethylvinylammonium bromide (TEVA) precursor with p-H_2 over $\mathbf{[Rh]_{aq}}$. However, no formation of TEA was observed in this case (some unidentified species were observed instead, Figure S14). Hydrogenation of ATPA over $\mathbf{[Rh]_{aq}}$ did not yield the desired tetrapropylammonium (TPA) as well (Figure S15). Likely, the increased steric hindrances impede hydrogenation of C=C bonds in TEVA and ATPA precursors over $\mathbf{[Rh]_{aq}}$, making other chemical processes more favorable. Therefore, while symmetric TEA and (likely) TPA possess longer ^{14}N longitudinal relaxation times, their hyperpolarization is challenging and requires further investigation of related chemistry.

To conclude, hyperpolarization of ^{14}N nuclei—the isotope of nitrogen with natural abundance of >99 %—was demonstrated. This was achieved via pairwise addition of parahydrogen to tetraalkylammonium salts with unsaturated vinyl or allyl moieties followed by subsequent polarization transfer to ^{14}N nuclei at a high magnetic field using PH-INEPT or PH-INEPT+ pulse sequence. Up to 760-fold ^{14}N NMR signal enhancement was achieved at 7.05 T, corresponding to 0.15 % ^{14}N polarization. The efficiency of this approach can be further increased by careful optimization of chemistry and physics of the process. In particular, one can identify more efficient hydrogenation catalysts providing higher polarization levels and greater selectivity toward the desired reaction products. Alternatively, deuteration of the substrate is expected to prolong ^{14}N hyperpolarization lifetime[28] while the use of other polarization transfer schemes (e.g., ESOTHERIC[19] RF pulse sequence or PH-INEPT modified with frequency-selective pulses[32,33]) may boost the efficiency of polarization transfer to ^{14}N. Moreover, other hyperpolarization techniques besides PHIP (in particular, dDNP and SABRE) can be potentially employed for hyperpolarization of ^{14}N nuclei.

Supporting Information

The authors have cited additional references within the Supporting Information.[37–48]

Acknowledgements

OGS thanks the Russian Science Foundation (grant 21-73-10105) for the support of PHIP experiments and PH-INEPT simulations. IVK thanks the Ministry of Science and Higher Education of the Russian Federation for access to NMR equipment. RVS is grateful for his SD Mines startup package. DAB and JX acknowledge funding from the Alexander von Humboldt foundation in the framework of Sofja Kovalevskaja Award. The authors thank Dr. Dudari B. Burueva for stimulating discussions. Open Access funding enabled and organized by Projekt DEAL.

Conflict of Interest

The authors declare no conflict of interest.

Data Availability Statement

The data that support the findings of this study are available from the corresponding author upon reasonable request.

Keywords: NMR spectroscopy · parahydrogen · ^{14}N NMR · hyperpolarization · PHIP

[1] J. Eills, D. Budker, S. Cavagnero, E. Y. Chekmenev, S. J. Elliott, S. Jannin, A. Lesage, J. Matysik, T. Meersmann, T.

© 2024 The Authors. Angewandte Chemie International Edition published by Wiley-VCH GmbH

15213773, 2024, 22, Downloaded from https://onlinelibrary.wiley.com/doi/10.1002/anie.202402877 by Universitätsbibliothek Mainz, Wiley Online Library on [24/04/2025]. See the Terms and Conditions (https://onlinelibrary.wiley.com/terms-and-conditions) on Wiley Online Library for rules of use; OA articles are governed by the applicable Creative Commons License

Prisner, J. A. Reimer, H. Yang, I. V. Koptyug, *Chem. Rev.* **2023**, *123*, 1417.
[2] J. H. Ardenkjær-Larsen, B. Fridlund, A. Gram, G. Hansson, L. Hansson, M. H. Lerche, R. Servin, M. Thaning, K. Golman, *Proc. Natl. Acad. Sci. USA* **2003**, *100*, 10158.
[3] S. J. Elliott, Q. Stern, M. Ceillier, T. El Daraï, S. F. Cousin, O. Cala, S. Jannin, *Prog. Nucl. Magn. Reson. Spectrosc.* **2021**, *126–127*, 59.
[4] C. R. Bowers, D. P. Weitekamp, *J. Am. Chem. Soc.* **1987**, *109*, 5541.
[5] T. C. Eisenschmid, R. U. Kirss, P. P. Deutsch, S. I. Hommeltoft, R. Eisenberg, J. Bargon, R. G. Lawler, A. L. Balch, *J. Am. Chem. Soc.* **1987**, *109*, 8089.
[6] J.-B. Hövener, A. N. Pravdivtsev, B. Kidd, C. R. Bowers, S. Glöggler, K. V. Kovtunov, M. Plaumann, R. Katz-Brull, K. Buckenmaier, A. Jerschow, F. Reineri, T. Theis, R. V. Shchepin, S. Wagner, P. Bhattacharya, N. M. Zacharias, E. Y. Chekmenev, *Angew. Chem. Int. Ed.* **2018**, *57*, 11140.
[7] R. W. Adams, J. A. Aguilar, K. D. Atkinson, M. J. Cowley, P. I. P. Elliott, S. B. Duckett, G. G. R. Green, I. G. Khazal, J. López-Serrano, D. C. Williamson, *Science* **2009**, *323*, 1708.
[8] O. G. Salnikov, D. B. Burueva, I. V. Skovpin, I. V. Koptyug, *Mendeleev Commun.* **2023**, *33*, 583.
[9] D. A. Barskiy, S. Knecht, A. V. Yurkovskaya, K. L. Ivanov, *Prog. Nucl. Magn. Reson. Spectrosc.* **2019**, *114–115*, 33.
[10] B. J. Tickner, V. V. Zhivonitko, *Chem. Sci.* **2022**, *13*, 4670.
[11] E. V. Pokochueva, D. B. Burueva, O. G. Salnikov, I. V. Koptyug, *ChemPhysChem* **2021**, *22*, 1421.
[12] K. V. Kovtunov, O. G. Salnikov, I. V. Skovpin, N. V. Chukanov, D. B. Burueva, I. V. Koptyug, *Pure Appl. Chem.* **2020**, *92*, 1029.
[13] M. Goldman, H. Jóhannesson, O. Axelsson, M. Karlsson, *C. R. Chim.* **2006**, *9*, 357.
[14] A. N. Pravdivtsev, A. V. Yurkovskaya, H. Zimmermann, H.-M. Vieth, K. L. Ivanov, *RSC Adv.* **2015**, *5*, 63615.
[15] H. Jóhannesson, O. Axelsson, M. Karlsson, *C. R. Phys.* **2004**, *5*, 315.
[16] E. Cavallari, C. Carrera, T. Boi, S. Aime, F. Reineri, *J. Phys. Chem. B* **2015**, *119*, 10035.
[17] T. Theis, M. L. Truong, A. M. Coffey, R. V. Shchepin, K. W. Waddell, F. Shi, B. M. Goodson, W. S. Warren, E. Y. Chekmenev, *J. Am. Chem. Soc.* **2015**, *137*, 1404.
[18] M. Haake, J. Natterer, J. Bargon, *J. Am. Chem. Soc.* **1996**, *118*, 8688.
[19] S. Korchak, S. Yang, S. Mamone, S. Glöggler, *ChemistryOpen* **2018**, *7*, 344.
[20] T. Theis, M. Truong, A. M. Coffey, E. Y. Chekmenev, W. S. Warren, *J. Magn. Reson.* **2014**, *248*, 23.
[21] S. Knecht, A. S. Kiryutin, A. V. Yurkovskaya, K. L. Ivanov, *Mol. Phys.* **2019**, *117*, 2762.
[22] M. G. Pravica, D. P. Weitekamp, *Chem. Phys. Lett.* **1988**, *145*, 255.
[23] S. Aime, R. Gobetto, F. Reineri, D. Canet, *J. Chem. Phys.* **2003**, *119*, 8890.
[24] J. Natterer, T. Greve, J. Bargon, *Chem. Phys. Lett.* **1998**, *293*, 455.
[25] V. P. Kozinenko, A. S. Kiryutin, S. Knecht, G. Buntkowsky, H.-M. Vieth, A. V. Yurkovskaya, K. L. Ivanov, *J. Chem. Phys.* **2020**, *153*, 114202.
[26] V. V. Zhivonitko, V.-V. Telkki, K. Chernichenko, T. Repo, M. Leskelä, V. Sumerin, I. V. Koptyug, *J. Am. Chem. Soc.* **2014**, *136*, 598.
[27] D. O. Zakharov, K. Chernichenko, K. Sorochkina, S. Yang, V.-V. Telkki, T. Repo, V. V. Zhivonitko, *Chem. A Eur. J.* **2022**, *28*, 1.
[28] L. B. Bales, K. V. Kovtunov, D. A. Barskiy, R. V. Shchepin, A. M. Coffey, L. M. Kovtunova, A. V. Bukhtiyarov, M. A. Feldman, V. I. Bukhtiyarov, E. Y. Chekmenev, I. V. Koptyug, B. M. Goodson, *J. Phys. Chem. C* **2017**, *121*, 15304.
[29] J. McCormick, S. Korchak, S. Mamone, Y. N. Ertas, Z. Liu, L. Verlinsky, S. Wagner, S. Glöggler, L.-S. Bouchard, *Angew. Chem. Int. Ed.* **2018**, *57*, 10692.
[30] A. P. Jagtap, L. Kaltschnee, S. Glöggler, *Chem. Sci.* **2019**, *10*, 8577.
[31] F. Reineri, A. Viale, S. Ellena, D. Alberti, T. Boi, G. B. Giovenzana, R. Gobetto, S. S. D. Premkumar, S. Aime, *J. Am. Chem. Soc.* **2012**, *134*, 11146.
[32] A. N. Pravdivtsev, F. Ellermann, J. B. Hövener, *Phys. Chem. Chem. Phys.* **2021**, *23*, 14146.
[33] A. B. Schmidt, A. Brahms, F. Ellermann, S. Knecht, S. Berner, J. Hennig, D. Von Elverfeldt, R. Herges, J. B. Hövener, A. N. Pravdivtsev, *Phys. Chem. Chem. Phys.* **2021**, *23*, 26645.
[34] D. B. Burueva, V. P. Kozinenko, S. V. Sviyazov, L. M. Kovtunova, V. I. Bukhtiyarov, E. Y. Chekmenev, O. G. Salnikov, K. V. Kovtunov, I. V. Koptyug, *Appl. Magn. Reson.* **2022**, *53*, 653.
[35] E. S. Kononenko, A. I. Svyatova, I. V. Skovpin, L. M. Kovtunova, E. Y. Gerasimov, I. V. Koptyug, *J. Phys. Chem. C* **2022**, *126*, 14914.
[36] L. Dagys, A. P. Jagtap, S. Korchak, S. Mamone, P. Saul, M. H. Levitt, S. Glöggler, *Analyst* **2021**, *146*, 1772.
[37] E. Schmidt, *Apoth. Ztg.* **1912**, *27*, 682.
[38] H. Guo, C. Jin, Q. Zhang, P. Pan, X. Shi, *Method for Catalytic Synthesis of Pseudoionone by Alkaline Solid-Supported Ionic Liquid* **2020**, CN111187152.
[39] D. G. Raut, O. Sundman, W. Su, P. Virtanen, Y. Sugano, K. Kordas, J.-P. Mikkola, *Carbohydr. Polym.* **2015**, *130*, 18.
[40] Y. Zhang, A. A. Tamijani, M. E. Taylor, B. Zhi, C. L. Haynes, S. E. Mason, R. J. Hamers, *J. Am. Chem. Soc.* **2019**, *141*, 8277.
[41] H. Hellmann, G. M. Scheytt, *Justus Liebigs Ann. Chem.* **1962**, *654*, 39.
[42] B. Chapman, B. Joalland, C. Meersman, J. Ettedgui, R. E. Swenson, M. C. Krishna, P. Nikolaou, K. V. Kovtunov, O. G. Salnikov, I. V. Koptyug, M. E. Gemeinhardt, B. M. Goodson, R. V. Shchepin, E. Y. Chekmenev, *Anal. Chem.* **2021**, *93*, 8476.
[43] G. R. Fulmer, A. J. M. Miller, N. H. Sherden, H. E. Gottlieb, A. Nudelman, B. M. Stoltz, J. E. Bercaw, K. I. Goldberg, *Organometallics* **2010**, *29*, 2176.
[44] H. L. Deng, X. S. Luo, Z. Lin, J. Niu, M. H. Huang, *J. Org. Chem.* **2021**, *86*, 16699.
[45] D. A. Barskiy, A. Pravdivtsev, *ArXiv* **2023**, DOI: 10.48550/arXiv.2308.15837.
[46] S. E. Korchak, K. L. Ivanov, A. V. Yurkovskaya, H.-M. Vieth, *Phys. Chem. Chem. Phys.* **2009**, *11*, 11146.
[47] Y. Terui, M. Ueyama, S. Satoh, K. Tori, *Tetrahedron* **1974**, *30*, 1465.
[48] Y. Terui, K. Aono, K. Tori, *J. Am. Chem. Soc.* **1968**, *90*, 1069.

Manuscript received: February 8, 2024
Accepted manuscript online: March 24, 2024
Version of record online: April 16, 2024

© 2024 The Authors. Angewandte Chemie International Edition published by Wiley-VCH GmbH

15213773, 2024, 22, Downloaded from https://onlinelibrary.wiley.com/doi/10.1002/anie.202402877 by Universitätsbibliothek Mainz, Wiley Online Library on [24/04/2025]. See the Terms and Conditions (https://onlinelibrary.wiley.com/terms-and-conditions) on Wiley Online Library for rules of use; OA articles are governed by the applicable Creative Commons License